

Document downloaded from:

<http://hdl.handle.net/10251/165763>

This paper must be cited as:

Viezza, C.; Mazzuca, R.; Machado, DC.; Forte, MMDC.; Gómez Ribelles, JL. (2020). A new waterborne chitosan-based polyurethane hydrogel as a vehicle to transplant bone marrow mesenchymal cells improved wound healing of ulcers in a diabetic rat model. *Carbohydrate Polymers*. 231:1-10. <https://doi.org/10.1016/j.carbpol.2019.115734>



The final publication is available at

<https://doi.org/10.1016/j.carbpol.2019.115734>

Copyright Elsevier

Additional Information

# ***A new waterborne chitosan-based polyurethane hydrogel as a vehicle to transplant bone marrow mesenchymal cells improved wound healing of ulcers in a diabetic rat model***

1

2 **Christian Viezzer<sup>a,b,d</sup>, Rafael Mazzuca<sup>d</sup>, Denise Cantarelli Machado<sup>d</sup>, Maria Madalena**  
3 **de Camargo Forte<sup>a</sup> and José Luis Gómez Ribelles<sup>b,c</sup>.**

4 <sup>a</sup>Department of Materials Engineering, Federal University of Rio Grande do Sul, Porto  
5 Alegre, RS, Brazil.

6 <sup>b</sup>Centre for Biomaterials and Tissue Engineering, Universitat Politècnica de València, 46022  
7 València, Spain.

8 <sup>c</sup>Biomedical Networking Research Center on Bioengineering, Biomaterials and  
9 Nanomedicine (CIBER-BBN), València, Spain.

10 <sup>d</sup>Cellular Therapy Laboratory, Biomedical Research Institute, Pontifical Catholic University  
11 of Rio Grande do Sul, Porto Alegre, RS, Brazil.

12

## 13 **Abstract**

14 Foot ulcers, a common complication of diabetes, can cause physical incapacity and are  
15 derived from several factors, including poor wound healing. New therapeutic strategies are  
16 needed to minimize this complication for the sake of patients' health. We therefore developed  
17 a new chitosan- polyurethane hydrogel membrane (HPUC) and the test results confirmed  
18 that HPUC present low cytotoxicity and improved wound healing when used with  
19 mononuclear bone marrow fraction cells in the diabetic rat model. The biodegradable  
20 hydrogels were produced in block copolymer networks with a combination of chitosan blocks  
21 and biodegradable polyurethane. The membranes were characterized by FTIR, <sup>13</sup>C-NMR  
22 and thermogravimetry. Swelling and hydrolytic degradation were also evaluated. The non-  
23 solubility of the membranes in good solvents and the chemical characterization confirmed  
24 that the network structure was formed between the PU and the chitosan through  
25 urea/urethane bonds. The findings confirm that the HPUC have interesting properties that  
26 make them suitable for wound healing applications.

27 **Keywords:** Chitosan, waterborne polyurethane, wound healing, stem cell therapy

## 29 **1. Introduction**

30 The diabetes mellitus (DM) group of metabolic diseases, whose main characteristic is their  
31 hyperglycemic status, can be caused by the lack of insulin, a deficit in the production or  
32 reception of this hormone, among other causes. This disease is associated with several  
33 complications such as nephropathies, retinopathies, cardiovascular diseases, ulcers and limb  
34 amputation. It is a major public health problem worldwide due to its high prevalence and  
35 morbidity (Tao, Shi, & Zhao, 2015). Recurrent infections are caused by reduced immunity, a  
36 phagocytic function associated with hyperglycemia and poor vascularization (Baltzis,  
37 Eleftheriadou, & Veves, 2014; Boulton, 2013; Dinh et al., 2012; Hilfiker, Kasper, Hass, &  
38 Haverich, 2011). Cell therapy with bone marrow mesenchymal stem cells has proved to be  
39 an effective tissue repair strategy. Although the pathways involved in this repair process have  
40 not been fully identified, it is known that transplanted cells release growth factors that  
41 modulate the immune response, organize tissues, promote angiogenesis and stimulate cell  
42 differentiation. Tissue engineering can aid in the regenerative process by developing new  
43 biomaterials that can regenerate wounds, prevent contractions and protect against infectious  
44 agents. The tissue repair process occurs in three distinct phases: inflammation, formation  
45 and remodeling of new tissue (Baltzis et al., 2014; Boulton, 2013; Dinh et al., 2012; Hilfiker  
46 et al., 2011). Besides mitigating the inflammatory process, effective wound healing dressings  
47 must have the following characteristics: wound adherence, histocompatibility, fluid loss  
48 control and sterility.

49 In tissue engineering applications, biopolymers are of great interest in the manufacture of  
50 three-dimensional supports for cell culture and transplant. Chitosan (CHS) has been shown  
51 to be a highly suitable biopolymer for these applications (Ching Ting Tsao et al., 2011; Hilmi  
52 et al., 2013; T. Jiang et al., 2010; Moise et al., 2012). In addition to its good biocompatibility  
53 and non-toxicity, CHS has properties of particular interest as a wound-healing dressing, such  
54 as antimicrobial activity and excellent hemostatis (Ouyang et al., 2018). However one of its  
55 limiting factors is that it is not soluble in most organic solvents, although it can be dissolved  
56 in diluted acid solutions, and this hinders its use in the manufacture of complex structures.  
57 Chitosan has reactive amine and hydroxyl side groups occurring in the polymer chains, which  
58 can be modified by derivatization (Andrade et al., 2011; Casettari et al., 2012; Merchant et  
59 al., 2014). Alkaline treatment has also been used to reduce its molecular weight, if required  
60 (Barikani, Honarkar, & Barikani, 2010). These characteristics make it versatile to being

61 modified by grafting specific side groups or complexing with other classes of polymers.  
62 Polyurethanes (PUs) synthesized in aqueous dispersion have recently attracted much  
63 attention due to their physicochemical properties and biocompatibility (X. Jiang et al., 2007;  
64 Rowlands, Lim, Martin, & Cooper-White, 2007; Wang, Ping, Chen, & Jing, 2006; Zuber, Zia,  
65 Mahboob, Hassan, & Bhatti, 2010). The polyester poly (DL lactide-co-glycolide) (PLGA) is  
66 the most frequently used polyester in the synthesis of PU-based biomaterials. It has been  
67 approved by the FDA for different applications and has been used for many years in the  
68 development of medical devices as well as in raw materials for the pharmaceutical industry.  
69 Another of its benefits is that its hydrolysis products can be uptaken in the cellular metabolic  
70 pathway (Jovanovic et al., 2010; Page et al., 2012).

71 Bioresorption of CHS takes place by the enzymatic degradation of the polymer chains,  
72 although this is a slow process and depends on the location of the implant. Our hypothesis  
73 is that combining chitosan in a block copolymer network with other polymers susceptible to  
74 hydrolytic degradation will allow fast degradation of the material in aqueous media while  
75 maintaining the hydrogel behavior characteristic of chitosan and its proven regeneration  
76 capacities. This hypothesis is based on previous works on polymer blends or block  
77 copolymers containing chitosan as one of the components (Ünlü, Pollet, & Avérous, 2018,  
78 Gámiz-González, Vidaurre, & Gómez Ribelles, 2017; Hu et al., 2012; Dunia M. García Cruz,  
79 Gomez Ribelles, & Salmerón Sánchez, 2008 ). The novelty of this work was synthesizing PU-  
80 chitosan hydrogel membrane (HPUC) by introducing the PLGA blocks into soft PU segments.  
81 The hydrogel was formed in two steps, with the reaction of PU prepolymer via aqueous  
82 dispersion with unmodified chitosan. In this way, we produced a hydrogel for wound healing  
83 by combining CHS and PLGA blocks in a block copolymer network. Thus, we took advantage  
84 of PLGA's hydrolysis properties to control degradation. After the physical and chemical  
85 characterization of the hydrogel membrane, a biocompatibility test was performed with bone  
86 marrow mononuclear cells (BMMNC) before evaluating the membrane combination as a  
87 wound-healing dressing and for BMMNC injections in a rat diabetic model. The promising  
88 results provided evidence that HPUC plus BMMNC may be used to enhance the wound  
89 healing process.

## 90 **2. Experimental**

### 91 **2.1. Materials**

92 Chitosan [poly-( $\alpha$ -1/4)-2-amino-2-deoxy-D-glucopyranose] was purchased from Sigma-  
93 Aldrich with viscosity-average molecular weight of 1500 kDa determined by Mark-Houwink  
94 equation using 0.1M CH<sub>3</sub>COOH/0.2M NaCl as a solvent system at 25°C and average  
95 deacetylation degree (DD) of 75% determined by first derivative UV spectrophotometry  
96 (Dunia Mercedes García Cruz, Salmerón-Sánchez, & Gómez-Ribelles, 2012).  
97 Hexamethylene diisocyanate (HDI), 2,2-bis(hydroxymethyl) propionic acid (DMPA),  
98 Triethylamine (TEA), Tin(II) 2-ethylhexanoate, (3S)-cis-3,6-Dimethyl-1,4-dioxane-2,5-dione  
99 (L-Lactide), 1,4-Dioxane-2,5-dione (glycolide) and Streptozocin were purchased from Sigma-  
100 Aldrich. All materials were used as received without further purification.

## 101 **2.2. Membranes preparation**

102 The hydrogel based on waterborne polyurethane-chitosan (HPUC) was obtained from a  
103 polyurethane prepolymer and chitosan. The PU prepolymer was obtained from a polyester  
104 diol, previously synthesized, HDI and DMPA. Chitosan was used as received.

### 105 **2.2.1. Synthesis of the polyester diol**

106 The poly(lactid-co-glycolide)diol (PLGAdiol) was synthesized according to Ivirico et al. (2009)  
107 (Escobar Ivirico, Salmerón-Sánchez, Gómez Ribelles, & Monleón Pradas, 2009), with some  
108 modifications for obtaining a polyester copolymer with Mn of 2000 Da, from a mixture of 50:50  
109 of lactid acid and glycolide. Briefly, for this purpose 0.06 mol of lactide and 0.06 mol of  
110 glycolide were reacted with 0.01 mol of ethylene glycol at 120°C for 4 hours at 23 mbar. After  
111 synthesis, the polymer was dissolved in acetone, precipitated in hexane under stirring and  
112 dried in a vacuum.

### 113 **2.2.2. Synthesis of the PU prepolymer**

114 All PU prepolymers were obtained at a ratio 2/1/1 of NCO groups in HDI / OH groups in  
115 PLGAdiol / OH groups in DMPA with 7% (wt%) of the internal emulsifier DMPA in relation to  
116 the polyester diol. The internal emulsifier was 100% neutralized with TEA. The amounts of  
117 PLGAdiol for each HPUC series are listed in Table 1. The reaction was carried out in a three-  
118 necked round bottom flask using the adequate amounts of the polyester diol PLGA, HDI,  
119 DMPA and Tin(II) 2-ethylhexanoate in 5 mL of dimethyl sulfoxide. The reaction proceeded at  
120 70 °C for 2h under N<sub>2</sub> atmosphere and magnetic stirring. TEA was then added to neutralize -  
121 COOH groups of DMPA, and the reaction medium stirred for 30 min.

122

### 123 **2.2.3. Synthesis of hydrogel based waterborne polyurethane-chitosan (HPUC).**

124 Chitosan (0.01 g/mL) was solubilized in a 1% acetic acid solution for 45 min at 40 °C in an  
125 ultrasonic bath. Before use, the Chitosan solution was filtered (45 µm filter) and transferred  
126 to an addition funnel. The Chitosan solution was added dropwise to the PU prepolymer  
127 solution under stirring at 70 °C. After homogenization, the final solution was cast in a  
128 poly(tetrafluor ethylene) Petri dish and kept in an air circulating oven at 60 °C for 24h to allow  
129 the cross-linking reaction and solvent evaporation. The membranes thus formed were  
130 washed by immersion in deionized water for three days, changing the water every day. The  
131 membranes were finally washed with acetone in a refluxing apparatus for 4 h and then dried  
132 in a vacuum at room temperature.

### 133 **2.3. Characterization of HPUC membranes**

134 Infrared spectroscopy was performed on a Perkin-Elmer Spectrum 100 FT-IR (ATR)  
135 spectrometer. Solid- state <sup>13</sup>C NMR was performed on an Agilent DD2 500MHz (11.7T) NMR  
136 spectrometer. Thermogravimetric analyses were conducted on a Mettler-Toledo  
137 TGA/SDTA851e –FL1600. The samples were heated from 30°C to 900°C at a 10 °C/min  
138 heating rate in an N<sub>2</sub> atmosphere (50ml/min).

### 139 **2.4. Solubility test and water uptake**

140 The dry samples were cut into pieces weighing around 50 mg. For solubility tests, the  
141 samples were immersed in each solvent in a vial and shaken at room temperature. The water  
142 uptake of the samples after being immersed for different times was evaluated as:

143

144  $S = [(M_f - M_i) / M_i] * 100$ , where:

145

146  $M_i$  is the weight of the dry sample at time  $t = 0$  s and  $M_f$  is the weight of the wet sample at  
147 immersion time  $t$ .

### 148 **2.5. Degradation test**

149 The dry samples were cut into pieces weighing around 50 mg and immersed in a vial with  
150 phosphate buffered saline, PBS (pH 7.4). The samples were placed in a shaking incubator at  
151 37 °C. Buffer was changed weekly. All tests were performed in triplicate. After the periods of  
152 evaluation, the samples were removed from the buffer, gently dried with a filter paper and

153 washed three times with deionized (DI) water and then dried in an oven for 24 hours at 60 °C  
154 and immediately weighed.

155 The degradation ratio was determined according to the following equation:

156

157  $W_l = [(W_f - W_i)/W_i]*100$  ; were:

158

159  $W_l$ = weigth loss,  $W_i$ = Initial dry weight,  $W_f$ = dry weight after time degradation,

160

161 The results shown are the average of 3 replica.

162

### 163 **Table 1**

164 Amounts of reactants for the synthesis of HPUC series.

	<b>NCO/OH 2:1:1</b>			
<b>Sample</b>	<b>PLGAdiol (g)</b>	<b>DMPA/PLGAdiol (wt%)</b>	<b>CS (g)</b>	<b>Swelling Capacity (wt%)</b>
HPUC1	0.25	7	0.75	1200
HPUC2	0.5		0.5	1800
HPUC3	0.75		0.25	2000

165

### 166 **2.6. In vitro and in vivo assay**

167 This study was published and approved by the Health Sciences Commission of the School  
168 of Medicine of the Pontifícia Universidade Católica do Rio Grande do Sul - PUCRS under  
169 number 6236, and also by the Committee on Ethics in the Use of Animals - PUCRS,  
170 registered under number 15/00469. All procedures and techniques used during the animal  
171 experimentation are in accordance with the regulation proposed in the Brazilian Guidelines  
172 for the Care and Use of Animals for Scientific Purposes, by the National Council for the

173 Control of Animal Experimentation (CONCEA, 2013) and the Ethics Committee for Use of  
174 Animals of PUCRS (CEUA).

### 175 **2.6.1. Mononuclear Bone Marrow Fraction isolation (BMMNCs)**

176 After euthanasia the donor animals were dissected and bone marrow was aspirated from the  
177 long bones. The aspirated material was placed in falcon tubes containing RPMI medium and  
178 was transferred to another tube containing FicollPaque (Histopaque 1119, Sigma Aldrich) and  
179 centrifuged at 400 g. The mononuclear cell layer was collected and washed with Dulbecco's  
180 Phosphate Buffered Saline (DPBS). Viability was then determined using the trypan blue  
181 exclusion method. The same procedure was used for the tissue regeneration assay.

### 182 **2.6.2. Cell culture**

183 The cytotoxicity assay was performed with the adherent cell fraction. The cells were cultivated  
184 until confluence in a 75 cm<sup>2</sup> cell culture flask containing Dulbecco's modified Eagle's medium  
185 (DMEM), supplemented with 10% of Fetal Bovine Serum (FBS), gentamicin (0.025 g/L and  
186 streptomycin/penicillin (0, 1 g/L) in humid atmosphere at 37 °C with 5% of CO<sub>2</sub>.

### 187 **2.6.3. MTT assay**

188 Cytotoxicity was evaluated according to ISO 10993-5, evaluating the mitochondrial function  
189 by tetrazolium salt reduction (MTT). The sample extracts were prepared in DMEM. After  
190 sterilization with ethanol, the HPUC membranes were washed by immersion in sterile Milli Q  
191 water three times and then once in DPBS and DMEM without FBS, immersed in DMEM  
192 medium for 24, 48 or 72 hours and incubated with stirring in a humid atmosphere at 37°C  
193 with 5% of CO<sub>2</sub>. DMEM medium was used as negative control and copper sulfate (0.1 g.mL<sup>-</sup>  
194 <sup>1</sup>) in DMEM medium as positive control. All membranes were cut to a size of 3 cm<sup>2</sup> and were  
195 incubated in 5 ml DMEM to allow the extraction. The BMMNCs suspension was adjusted and  
196 seeded at a density of 0.5 x10<sup>4</sup> cell per well onto 96-well culture plates and incubated for 24  
197 hours to allow cellular adhesion. The cells were then incubated for 24 h with DMEM and after  
198 that, the reading was performed. The absorbance values obtained were normalized by  
199 negative control with 100% viable cells. All the tests were performed in triplicate.

### 200 **2.6.4. Direct contact**

201 The cells were seeded at a density of 5 x 10<sup>4</sup> cells per well onto a 24-well culture plate. The  
202 membrane was cut into a small circle (11-mm diameter) and placed in the middle of a well  
203 and incubated for 24 hours, 48 hours and 72 hours in humid atmosphere at 37°C with 5% of



204 CO<sub>2</sub>. Cell viability was evaluated by the Live/Dead Cell Viability Assay on an Inverted Phase  
205 Contrast Fluorescence Microscope (Thermo Fischer Scientific) according to the  
206 manufacturer's instructions.

### 207 **2.6.5. Animal model of diabetic ulcers**

208 60 day-old adult female Wistar rats weighing between 200 and 300g were given water and  
209 food ad libitum. Tail blood was collected at time 0 to evaluate the glycemic levels. All animals  
210 were fasted for 8 hours prior to diabetes induction, which was by an intraperitoneal injection  
211 of Streptozocin (70 mg/kg). Seven days after the streptozotocin injection the blood glucose  
212 levels of the animals were measured by the Accu-Check Active kit (Roche Diagnostics  
213 GmbH). The animals with blood glucose levels above 250mg/dL were considered diabetic.  
214 After glucose measurement, the animals were divided into two groups as described below.  
215 The animals submitted to the simulated ulcer procedure were given anesthesia of 80%  
216 Ketamine and 20% Chlorpromazine, followed by a dorsal incision of about 6mm diameter  
217 with a scalpel to simulate an ulcer wound.

### 218 **2.6.6. Experimental Design and Treatment of Groups**

219 In the *in vivo* evaluation for minimizing the use of animals, only HPUC1 membrane was  
220 selected because it is less fragile than HPUC2 and HPUC3 because its water sorption  
221 capacity is smaller while cytotoxicity results were similar in the three samples (see below) .  
222 The 16 rats were divided into 2 groups: Group 1 (control) (n=8): diabetic animals, with a  
223 wound, without treatment; Group 2 (n=8): diabetic animals with HPUC and BMMNCs  
224 transplanted onto the wound site. After the formation of the wound,  $1 \times 10^6$  cells of the  
225 mononuclear bone marrow fraction were transplanted into each animal in Group 2 by injection  
226 into the edge of the wound. After this procedure, the HPUC was positioned and sutured onto  
227 the wound. The animals were evaluated histologically in two different periods of time: 7 and  
228 14 days after membrane implantation.

### 229 **2.7 Histopathology of diabetic mice wounded skin tissues**

230 Samples obtained from the histological analyses of the wound were removed 7 and 14 days  
231 after wound formation. To obtain the sample, the wounded area was removed from the  
232 animals backs after euthanasia in the CO<sub>2</sub> chamber. All the samples were fixed in neutral  
233 buffered formalin and embedded in paraffin wax. Each section was 4µm thick and stained  
234 with hematoxylin-eosin (H&E). The analysis of the epithelial tissue and the depth of the  
235 epithelial cell-covered wound were considered. The analysis of connective tissue was

236 considered for the study of the inflammatory process, measured by the type and quantity of  
237 inflammatory cells and presence / absence of fibrosis, using H&E staining. The analyses were  
238 performed by two blinded examiners, previously instructed by a pathologist and calibrated by  
239 the kappa coefficient test.

## 240 **2.8. Macroscopic wound closure analyses**

241 The closure of the wounds was measured by comparing with ImageJ software the images  
242 recorded during the experiments. The formula used to measure the wound regeneration rate  
243 was as follows:

244

245  $RWA = (DA)/(OWA)*100$ ; were:

246

247 RWA: Residual wound área (%), DA: Detected Area, OWA: Original Wound Area.

248

## 249 **2.9. Statistical Analysis**

250 Quantitative data was expressed as mean  $\pm$  standard deviation. To compare the regeneration  
251 of the wound between the groups, an unpaired t test was performed at each time to compare  
252 the difference in wound closures. Values with  $p < 0.05$  were considered statistically significant.  
253 All the statistical analyses were performed with the statistical GraphPad Prism.

## 254 **3. Results and discussion**

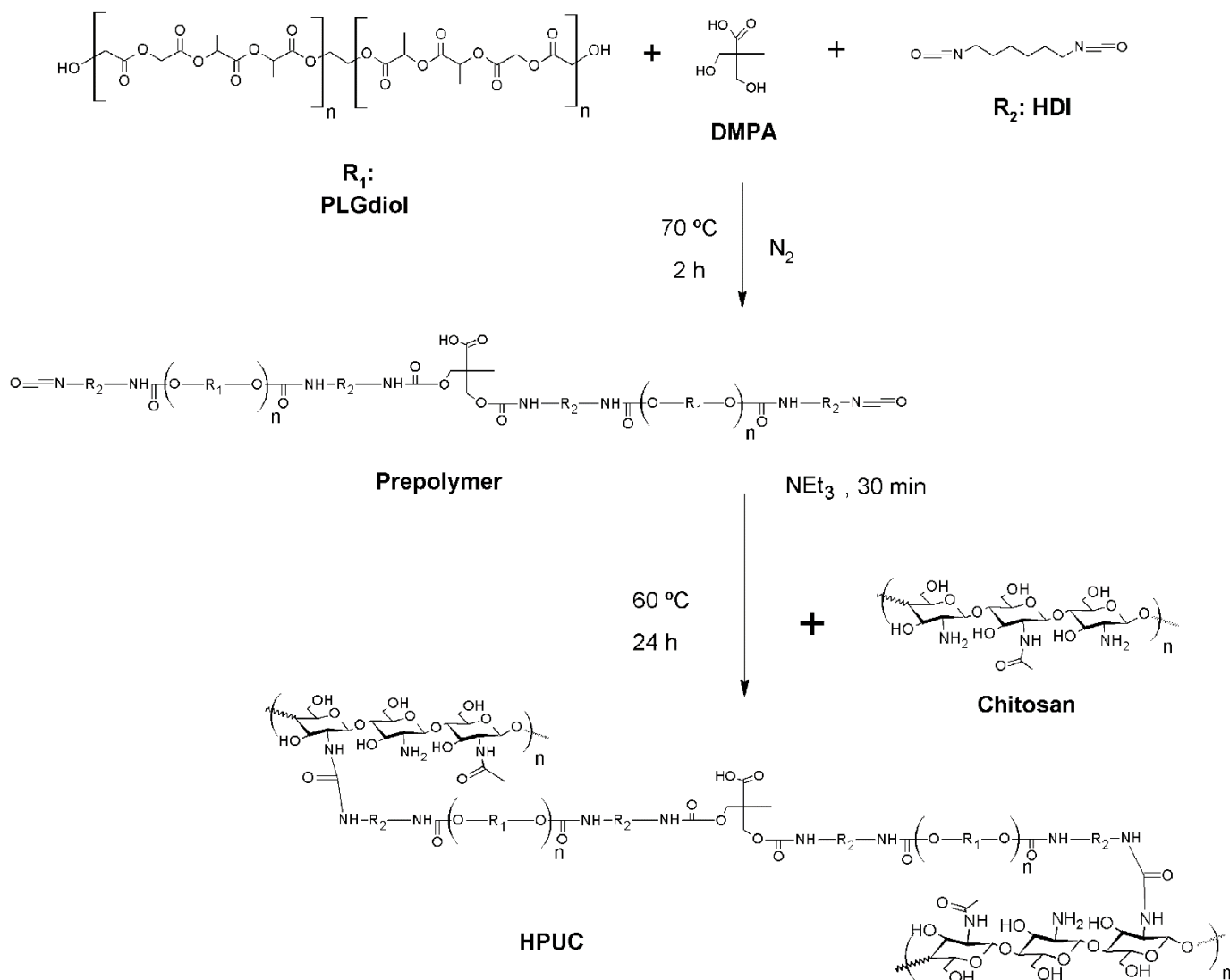
### 255 **3.1 Synthesis of hydrogel membranes**

256 The chitosan waterborne polyurethane was obtained in two stages as shown in the reaction  
257 scheme in Figure 1. The first (i) step consisted of the synthesis of the polyurethane  
258 prepolymer (PU prepolymer) with different weights of the soft segment poly (lactide-co-  
259 glycolide) diol, with HDI and DMPA as a chain extensor. In the second (ii) step, the HPUC was  
260 obtained by crosslinking reaction of the PU prepolymer with chitosan during membrane  
261 formation.

262 The synthesized membranes to be used as wound dressings were successfully obtained as  
263 shown in Figure 1. However, the membrane (HPUC3) with the highest amount of prepolymer  
264 (75%) became more brittle than the others (Figure S1 in Supplementary Material). This could  
265 have been due to the membrane presenting a phase separation, which may have contributed

266 to the immiscibility of the components and making it brittle ( $T_g$  15 °C, data not shown). This  
267 was not observed in the other two membranes.

268



269

270 **Fig. 1.** Synthesis route of the HPUC membranes.

271

### 272 3.2. Swelling

273 Chitosan was soluble in acetic acid 1% while the prepolymers were soluble in DMSO, acetone  
274 and  $CHCl_3$ . The membranes were not soluble in the solvents used to solubilize the  
275 prepolymer or in acetic acid 1%, proving the formation of crosslinked networks. Sample  
276 weight in immersion in liquid water stabilizes after 48 hours (See Figure S2 in Supplementary  
277 Material). The water sorption capacity at 48 hours for the different samples is larger than  
278 1000% measured on dry basis (Table 1). The network swelling capacity confirms that,

279 contrary to what could be expected, the membrane with the highest hydrophobous  
280 component, HPUC3, had the highest water uptake. The water content measured at 48 hours  
281 of immersion time thus fell from about 2000 to 1200 when the PLGA content was reduced  
282 from 75% to 25% (samples HPUC3 and HPUC1). The figure does not show a curve for pristine  
283 chitosan because it is water soluble, since the amine groups remain protonated after  
284 dissolution in the acidic medium. Hydrogel equilibrium water content is described by the Flory  
285 Rehner Equation (Flory & Rehner, 1943), which shows that swelling increases with a  
286 favorable water-polymer segment interaction parameter and with the higher average  
287 molecular weight between crosslinks in the network, i.e. with a reduced crosslinking density.  
288 The higher PLGA/CHS ratio should yield a less favorable average interaction parameter  
289 between PU soft segments and water. The fact that swelling capacity nevertheless increases  
290 could be due to less efficient crosslinking with the presence of a significant number of  
291 unreacted carboxyl end groups in PU prepolymer.

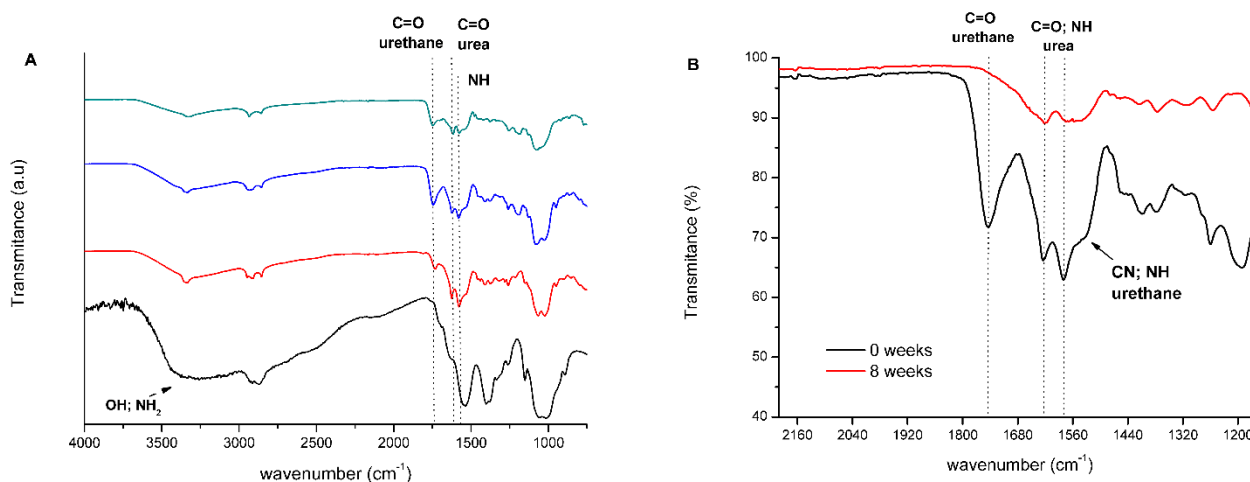
### 292 **3.3. FT-IR of chitosan polyurethane.**

293 The spectra of original chitosan and polyurethane based on chitosan with different soft  
294 segment contents are shown in Figure 2A.

295 The chitosan spectrum shows the typical large peaks in the 3340  $\text{cm}^{-1}$  region relative to the  
296 stretching of the OH and  $\text{NH}_2$  groups, 2872-2920  $\text{cm}^{-1}$  to  $\text{CH}_2$  stretch, 1151  $\text{cm}^{-1}$  for C –O  
297 –C of the chitosan ring. The appearance of the peaks relative to urea and urethane bonds  
298 can be observed in the case of polyurethane prepolymer and the networks. The membrane  
299 formed has two hard segments due to the urea and urethane bonds formed between the  
300 diisocyanate groups and  $\text{NH}_2$  and OH chitosan groups and PLGA/DMPA, respectively  
301 (Subramani, Park, Lee, & Kim, 2003). These urethane bond peaks appear in the 1730-1746  
302  $\text{cm}^{-1}$  region (C=O stretch), 1027-1074  $\text{cm}^{-1}$  (C-O stretch) and urea bonds at 1616 -1625  $\text{cm}^{-1}$   
303 (C=O stretch), 1589  $\text{cm}^{-1}$  (NH bending) and 1254 – 1260  $\text{cm}^{-1}$  (C-N stretch). As found by  
304 other authors, the urea bond formation (-NHCONH-) occurs because the preferential  
305 reactivity of NCO groups with  $\text{NH}_2$  groups is much more reactive than the OH groups (S. H.  
306 Chen et al., 2012; Pérez-Limiñana, Arán-Aís, Torró-Palau, Orgilés-Barceló, & Martín-  
307 Martínez, 2005; Velazquez-Morales, Le Nest, & Gandini, 1998).

308 In the supplementary data, Figure S3, the FTIR spectra of the synthesized PLGAdiol and the  
309 PU prepolymer are shown. Although is observed an overlapping in the urethane and urea  
310 absorption region the peaks around 1600-1750  $\text{cm}^{-1}$  are distinguishable. The presence of

311 the absorption band at 1625 cm<sup>-1</sup>, which is ascribed to hydrogen-bonded urea groups  
 312 (Marchant, Zhao, Anderson, & Hiltner, 1987; Zhang, Ren, He, Zhu, & Zhu, 2007) and is  
 313 absent in the prepolymer is slightly different in the networks with varying composition,  
 314 showing that sample composition affects the reaction mechanism.



315

316

317 **Fig. 2.** FTIR spectrum of membranes. (A) Membranes before the degradation test. Arrows  
 318 and lines indicate the main groups related to crosslinking between the prepolymer PU and  
 319 CHS (in black: CHS, red: HPUC1, blue: HPUC2 and green: HPUC3). (B) Membrane  
 320 HPUC2 after 8 weeks immersion in PBS 1x buffer.

321

### 322 3.4. Solid state <sup>13</sup>C-NRM

323 Figure 3 shows the solid state NRM spectra of chitosan and HPUC membranes with 25%  
 324 (HPUC1), 50% (HPUC2) and 75% (HPUC3) soft segment. In chitosan the peaks in Figure 3  
 325 are those of C1 ( $\delta$ 104.8), C4 ( $\delta$ 81.5), C5 and C3 ( $\delta$ 75.1), C6 and C2 ( $\delta$ 57.2), and CH3 ( $\delta$ 22.6),  
 326 in agreement with other studies (de Moura, Aouada, & Mattoso, 2008; Heux, Brugnerotto,  
 327 Desbrières, Versali, & Rinaudo, 2000). For HPUC membranes we observed novel peaks,  
 328 which have been reported as the chitosan-PU crosslinking for HPUC1 peaks:  $\delta$ 174.82,  
 329  $\delta$ 159.27,  $\delta$ 99.49,  $\delta$ 73.24,  $\delta$ 60.60,  $\delta$ 41.65,  $\delta$ 29.50,  $\delta$ 17.34; for HPUC2:  $\delta$ 176.77,  $\delta$ 159.76,  
 330  $\delta$ 101.92,  $\delta$ 73.24,  $\delta$ 61.09,  $\delta$ 41.65,  $\delta$ 29.98,  $\delta$ 16.86 and HPUC3:  $\delta$ 174.34,  $\delta$ 159.27,  $\delta$ 102.40,  
 331  $\delta$ 74.40,  $\delta$ 60.60,  $\delta$ 42.13,  $\delta$ 30.64,  $\delta$ 23.13. The carbonyl (CO) shifts are far from the field (155-  
 332 210 ppm) and generally weak due to slow relaxation. For urea and urethanes the shifts are  
 333 170-180 and 150-160, respectively. The peak of <sup>13</sup>C spectra in the urea group occurs at a

334 higher magnetic field than those in the urethane group (Zhang, Cheng, & Hu, 2003)□. The  
335 displacement, found in HPUCs around  $\delta 174$ , is related to urea bounds between  $-\text{NH}_2$  groups  
336 of chitosan and  $-\text{NCO}$  groups of PU prepolymer, while  $\delta 159$  is related to both urethane bonds  
337  $-\text{NHCOO}-$  of polyester and DMPA in the soft and hard segments, respectively (Barikani et al.,  
338 2010; Leventis et al., 2010)□.

339

340

341

342

343

344

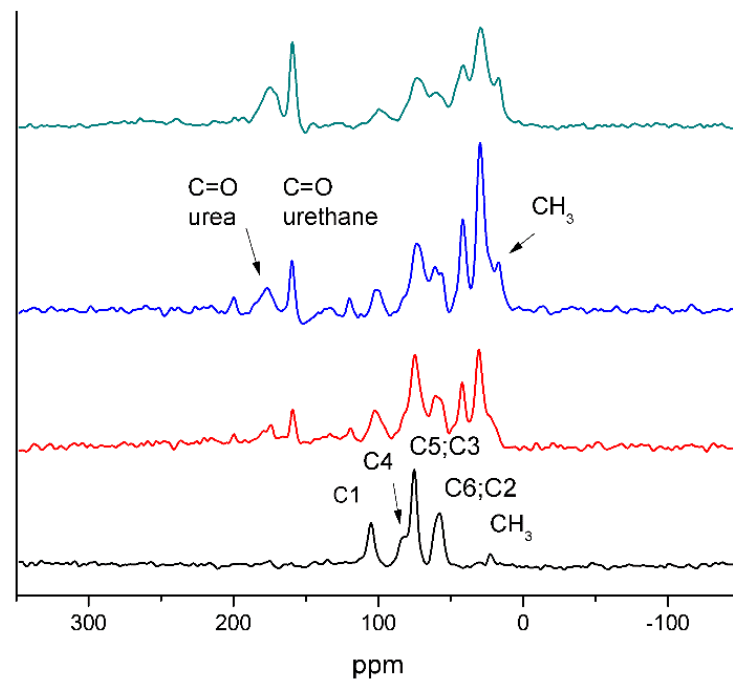
345

346

347

348

349



350 **Fig. 3.** Solid state  $^{13}\text{C}$ -NRM spectrum of membranes. Arrows indicate the main shifts  
351 related to crosslinking between the prepolymer PU and CHS (in black: CHS, red: HPUC1,  
352 blue: HPUC2 and green: HPUC3).

### 353 3.5 Thermogravimetric analysis

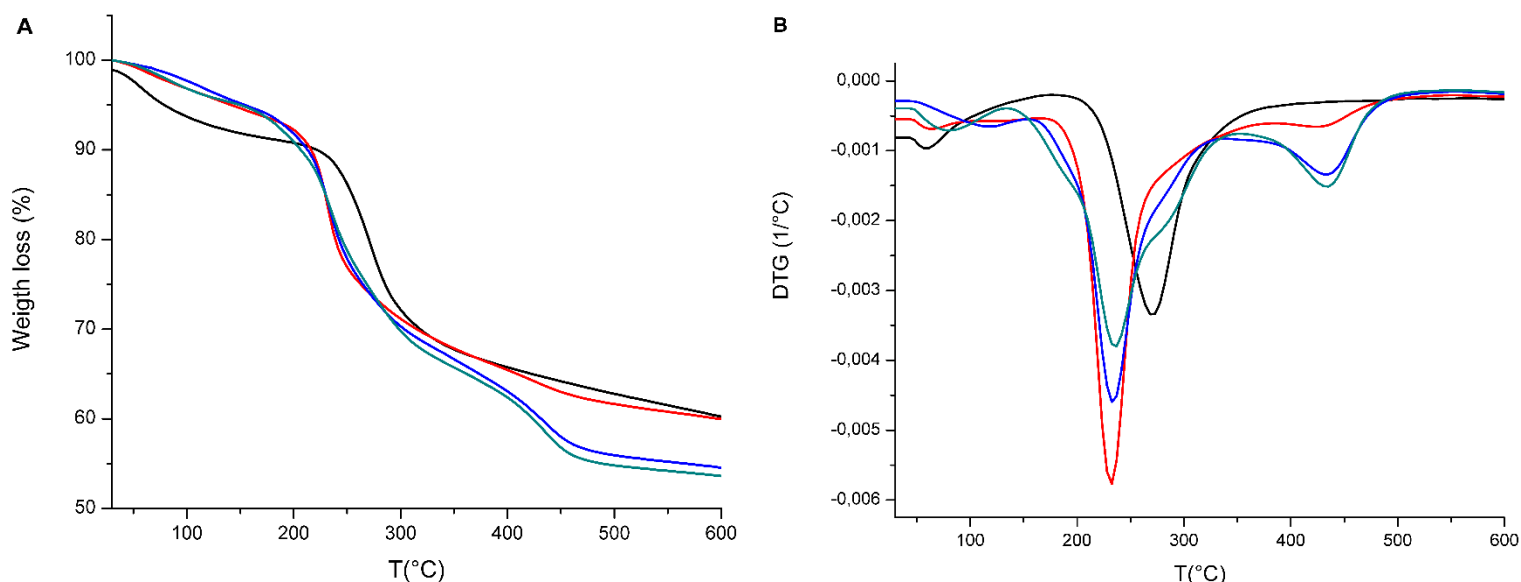
354 Figure 4B show the derivative weight loss (DTG) curves of chitosan and HPUC membranes.  
355 In the chitosan and HPUC TG curve we observed the first thermal event in the 40-140°C  
356 range, which indicates a weight loss of less than 6% attributed to the evaporation of residual  
357 water from the polymer (de Britto & Campana-Filho, 2007)□. The second thermal event,  
358 after 140 °C, is due to the overlapping of the degradation of chitosan and PLGA chains.  
359 Thermal degradation of the chitosan used in this study takes place in the 187-372 °C range  
360 (with a maximum in the DTG plot at 268 °C) and is attributed to the thermal decomposition of  
361 chitosan chains (Abused et al., 2014; Neto et al., 2005; Zawadzki & Kaczmarek, 2010)□. For  
362 HPUCs, thermal decomposition in the TG curve occurs in a broader temperature range

363 between 142 and 502°C. The overlap of the different phenomena can best be seen in the  
364 DTG curve (Figure 4B).

365 The peak appearing at the lower temperature is attributed to the degradation and weight loss  
366 of the hard and soft segments of the urethane groups (the intensity of this peak increases  
367 with increasing PLGA content, as expected). This peak appears at temperatures lower than  
368 that of pure chitosan degradation (the maximum in DTG curve appears at ~235°C). On the  
369 high temperature side of this peak, in the chitosan degradation temperature range a shoulder  
370 can be seen indicating the decomposition of chitosan chains in the network. The highest  
371 temperature peak in the HPUCs is relative to the weight loss of the hard segment of the urea  
372 bond, since the energy of the urea bond is larger than that of the urethane bond, the  
373 degradation peak in urea appears at higher temperatures (García-Pacios, Costa, Colera, &  
374 Martín-Martínez, 2011). Table 2 gives the chitosan and HPUC thermal data. HPUC  
375 membranes had a lower onset temperature, HPUC1> HPUC2> HPUC3, with PLGA  
376 incorporated in the chitosan structure, which could be associated with changes in the  
377 intermolecular interactions between polysaccharide chains resulting in reduced polymer  
378 thermal stability.

379

380



381 **Fig. 4.** Graphs of the relative weight loss curves (A) and derived weight loss (B) of chitosan  
382 membranes and HPUCs (in black: CHS, red: HPUC1, blue: HPUC2 and green: HPUC3).

383

384 **Table 2**

385 Maximum degradation temperature of CHS and HPUCs.

Sample	Temperature range °C	Second Stage T <sub>max</sub> (°C)	Third Stage T <sub>max</sub> (°C)	Weight loss %
CHS	187-372	268		30
HPUC1	171-476	232.5	426	36
HPUC2	151-507	232.5	435	40
HPUC3	142-507	237	435	41

386

387 **3.6. Degradation in PBS medium**

388 Figure 5 shows the degradation curves in an aqueous solution (PBS 1x pH 7.4) for up to eight  
389 weeks. There is a significant mass loss at the end of the eight weeks in the HPUC2 and  
390 HPUC3 samples, 87.0% and 90.5% respectively, compared to 56.4% for HPUC1 and 53.2%  
391 for CHS. The findings show that membrane weight loss has two different mechanisms. Since  
392 the membranes were not neutralized at the end of the synthesis, one could expect that the  
393 chitosan chain amine groups would remain protonated and that the chitosan would be slowly  
394 dissolved in the aqueous solution. Thus, the pure chitosan film presents a continuous weight  
395 loss of up to 53.2%, which cannot be explained by hydrolysis. This delivery of chitosan chains  
396 by dissolution in the aqueous medium is prevented in the HPUC hydrogels by the polymer  
397 network structure. Nevertheless, HPUC2 and HPUC3 membranes can degrade by nearly  
398 100% in eight weeks. Since cleavage of chitosan chains by hydrolysis does not take place in  
399 the degradation times of our experiments, we hypothesize that the cleavage of the PLGA  
400 chains and urea linkages liberates chitosan chains that are susceptible to being dissolved in  
401 the medium, since they are protonated, contributing to the weight loss (See the schema in  
402 Figure S4 of supplementary material).

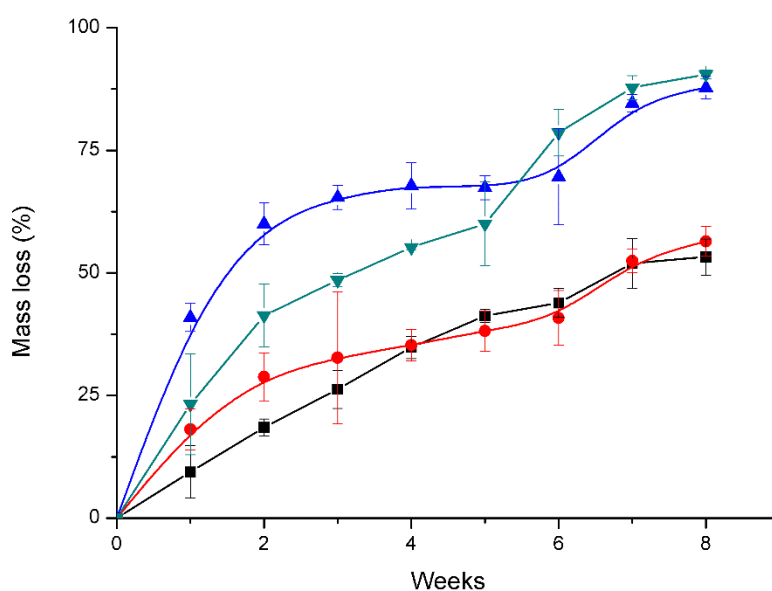
403 FTIR analysis support this assumption. After eight weeks of degradation of the HPUC  
404 membranes (Figure 2B) it is clear the disappearance of the peaks characteristic of the PU



405 regions between 1500-1150  $\text{cm}^{-1}$ , and the strong band at approximately 1745  $\text{cm}^{-1}$   
406 corresponding to a C = O bond of ester groups showing the degradation of the PLGA segment.  
407 In addition, the original position of the amide peak at 1579  $\text{cm}^{-1}$  (C-N and N-H) moves to  
408 1575  $\text{cm}^{-1}$  (Figure 2B). It is also possible to visualize the displacement of the 1625  $\text{cm}^{-1}$   
409 peak for 1619  $\text{cm}^{-1}$  corresponding to the carbonyl bond in the urea groups (C = O amide I)  
410 indicating degradation of the rigid segment ((Marcos-Fernández, Abraham, Valentín, &  
411 Román, 2006; Pretsch, Jakob, & Müller, 2009), the same can be seen in the 1530  $\text{cm}^{-1}$  region  
412 referring to PU urethane group bound to the CHS chains.

413 The high swelling capacity of the HPUC network, even for the largest PLGA content,  
414 contributes to the hydrolysis process. PLGA chains are exposed to water molecules in the  
415 swollen sample and thus the hydrolysis of the ester groups is faster than in bulk PLGA which  
416 is highly hydrophobous.

417 Thus, we propose that the fast, and nearly complete degradation of the HPUC hydrogels is  
418 due to the combination of the loose of the degradation fragments of PLGA chains together  
419 with the delivery of CHS chains detached from the network structure.



430 **Fig. 5.** CHS and HPUC mass loss curves after up to eight weeks: ■ CHS, ● HPUC1,  
431 ▼ HPUC2 and ▲ HPUC3. All values are expressed as mean  $\pm$  standard deviation (n=3).

432  
433

### 434 **3.7. In vitro cytotoxicity analysis of HPUC membranes**

435 To select the best membrane to continue the *in vivo* assay we evaluated cellular viability by  
436 mitochondrial metabolic activity. For the indirect cytotoxicity analysis, the adherent BMMNCs  
437 were cultured with membrane extracts obtained after immersion of the membranes for  
438 periods of 24, 48 and 72 hours. The viability of the cells cultured in direct contact with HPUC  
439 membranes in the same time periods was assessed with a live/dead test with fluorescence  
440 microscopic evaluation. In all the exposure periods in the indirect contact experiment the  
441 viability was of all the membranes above 80% of the negative control (Figure S5 in  
442 Supplementary Material)

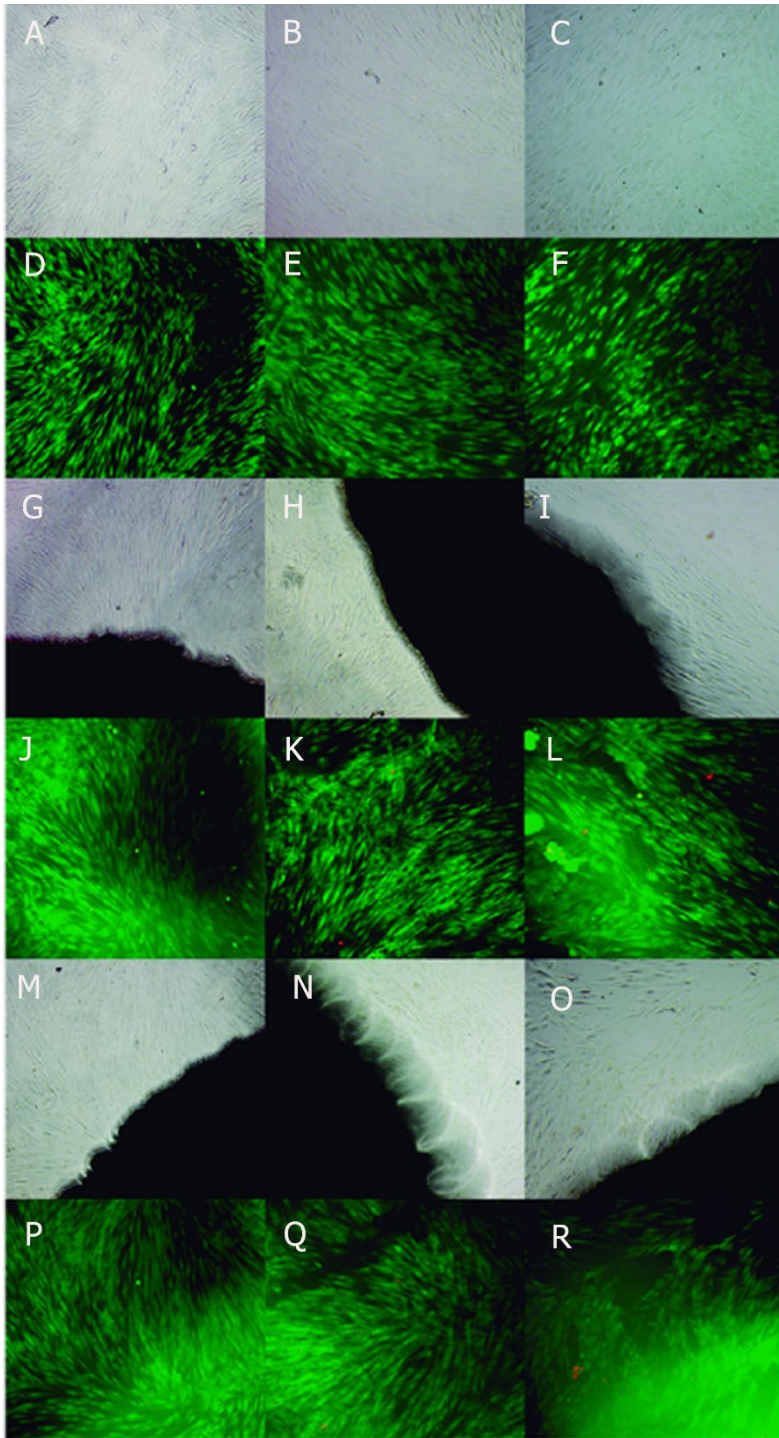
443 Considering the results obtained for HPUC3 degradation time and brittleness in the swelling  
444 experiments, we opted for HPUC1 and HPUC2 membranes to continue the evaluation. The  
445 HPUC1 and HPUC2 networks were analyzed in direct contact using the live/dead  
446 fluorescence assay, which provides information on physical cell properties (cellular  
447 membrane integrity) and biochemical intracellular esterase activity (Masson-Meyers, Bumah,  
448 & Enwemeka, 2016). No cytotoxicity effect was detected (see images in Figure 6), indicating  
449 that the cells produced esterase (green fluorescence), which is an indicator of viable cells,  
450 while the red fluorescence that indicates cell death is rarely observed. The images show the  
451 cells well spread out on the culture plate, while the morphology and cell numbers are quite  
452 similar to those of the controls.

### 453 **3.8. HPUC plus BMMNCs accelerated wound repair in diabetic rats**

454 Considering the high costs of treating patients with ulcers in the lower limbs, and the high  
455 morbidity and mortality rate caused by this type of wound, the research for new treatments is  
456 necessary. Diabetic patients affected by ulcers in the lower limbs go through a prolonged  
457 inflammatory phase during tissue regeneration, with persistence of a pro-inflammatory profile,  
458 moving from an acute to a chronic state. This prolonged inflammation is directly related to the  
459 precarious healing of these wounds, leading these individuals to recurrent infections, and  
460 when not properly treated at an early stage, can lead to amputation. Our study aimed to  
461 identify whether the use of a biological dressing associated with mononuclear bone marrow  
462 fraction cells from rats would be able to improve the regenerative response in ulcerous  
463 wounds in diabetic rats.

464 From an intraperitoneal use of streptozotocin, it was possible to establish an animal model of  
465 diabetes. After the model was established, we were able to create a wound on the animals'

466 backs to simulate an ulcer wound, simulating the ulcer shown in lower limbs from diabetic  
467 individuals. From the results, it was observed that the group of animals treated with the HPUC  
468 combined with the injection of BMMNCs in the interphase between the tissue and the HPUC  
469 membrane (Group 2) showed significantly better results in terms of healing in the first 7 days  
470 after the formation of the wound compared to the control group (Figure 7). During the first few  
471 days, we observed that the animals that had the HPUC plus BMMNCs on the wound had a  
472 cleaner and drier wound, when compared macroscopically with the animals that did not  
473 receive the treatment. This suggests that the membrane achieved hemostasis of the wound,  
474 supporting the formation of the fibrin matrix and cell infiltration (Eming, Martin, & Tomic-canic,  
475 2014; Oberyszyn, 2008).



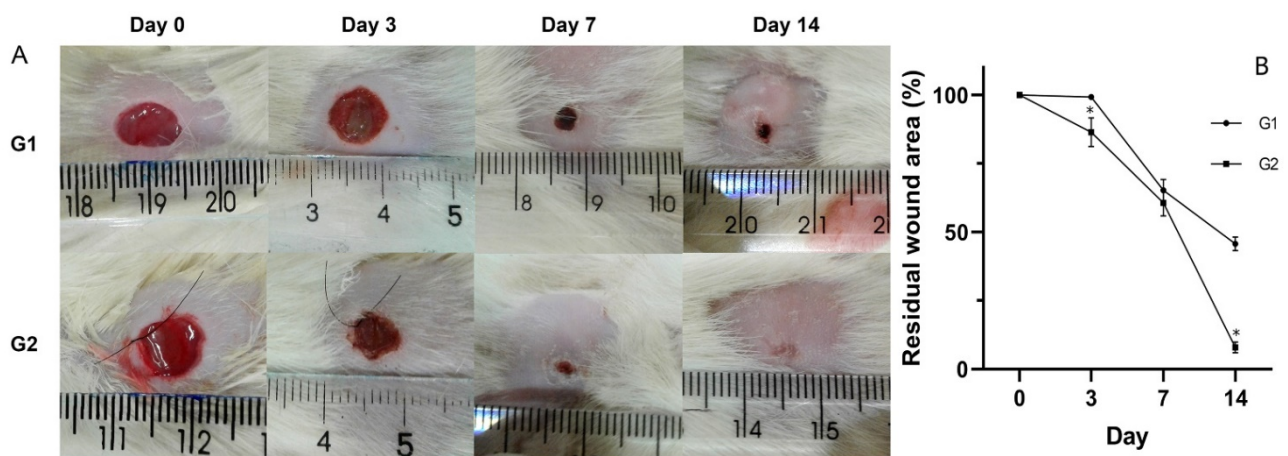
476

477

478 **Fig. 6.** Representative fluorescent image of MSCs: (A – F) Control, (G– M), HPUC2, (N –  
 479 **S)** HPUC1. Live cells were stained with calcein AM (green) using a FITC filter and dead  
 480 cells were stained with Ethidium homodimer (red) and captured by an PI filter. All images  
 481 were acquired after 24, 48 and 72 hours. Magnification 100x.

482 In addition, the animals treated with the BMMNCs plus the biomaterial showed a significantly  
483 better regeneration rate than those from the control group after 14 days, with a significant  
484 reduction in wound size.

485 The use of bone marrow-derived mesenchymal cells enhances tissue regeneration,  
486 significantly reducing the wound size in rat diabetes ulcer models using streptozotocin. In  
487 addition, complete wound healing time was also significantly lower in the mesenchymal cell  
488 treated group (Kuo et al., 2011). The combination BMMNCs and HPUC provided wound  
489 healing in just 14 days (wound closure >90%). Although previous studies in the literature with  
490 different biomaterials showed a significant improvement of wound healing, they required  
491 longer times and a more intense inflammatory process (Ahmed et al., 2018; Sayed et al.,  
492 2016). The macroscopic analysis of wounds treated with these membranes revealed a  
493 considerably smaller wound bed than those in the control group.



494

495

496 **Fig. 7.** Representative image in the effects of HPUC1 and BMMNCs on wound healing in  
497 diabetic ulcer model. (A) Macroscopic observations in wound areas in the control (G1) and  
498 wound healing contraction induced by HPUC1 plus BMMNCs (G2). (B) Residual wound area.  
499 The results are expressed as mean  $\pm$  standard deviation (n= 6). (\*) indicates significant  
500 difference,  $p < 0.05$ .

501

### 3.9. Histological wound healing by H&E staining

502

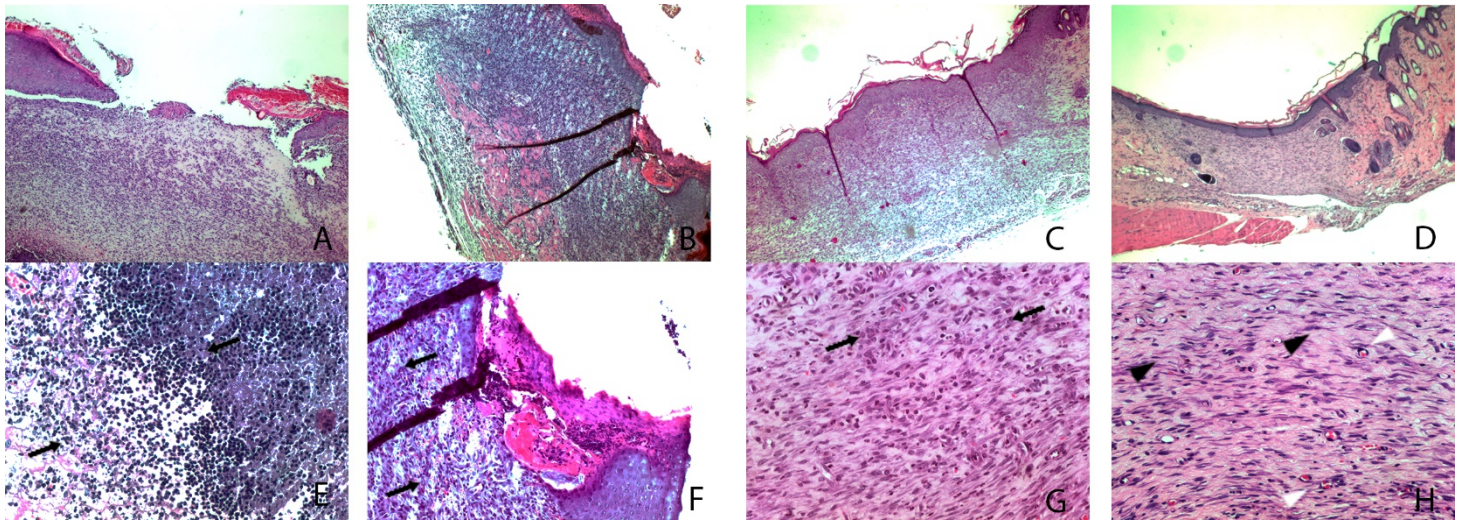
To evaluate the role of BMMNCs in the remodeling and speed of tissue regeneration when  
503 transplanted with a HPUC membrane, we collected the samples from the wound region in  
504 the diabetic rats for histological analysis on days 7 and 14. On day 7 it was observed a



505 noticeable difference on wound closure from the treated group (Figure 8) compared to the  
506 non-treated group.

507

508



509

510 **Fig. 8.** Representative histologic analysis of the wound region. Tissue samples were  
511 collected on day 7 (**A, E, C, G**) and 14 (**B, F, D, H**). H&E staining showed severe  
512 inflammation in the control group (**A, B, E, F**) and wound healing and re-epithelialization (**C,**  
513 **D, G, H**) in the HPUC1 plus BMMNC group. Black arrows indicate inflammatory cell  
514 infiltrate, black arrowhead fibroblasts and white arrowhead indicate blood vessels.  
515 Magnification 4x in A, E, C, D, and 20x in B, F, G, H.

516

517 Unlike Group 2 (HPUC + BMMNCs), Inflammatory cell infiltrate was observed in the control  
518 group and there were no signs of epithelial regeneration. In Group 2, moderate inflammatory  
519 infiltrate was visible, together with wound closure with epithelization. On day 14 remodeling  
520 of the wound was clearly seen in Group 2 with organized connective tissue and  
521 neovascularization, indicating successful healing. This was not found in the control group.

522 Initial inflammation at the beginning of healing is critical for the regeneration period, which  
523 dictates the second phase of wound regeneration, with reduced inflammation remodeling and  
524 culminating in wound closure (Koehler, Brandl, & Goepferich, 2018)□. All these processes  
525 involve several cell types. The mesenchymal cells in the BMMNC fraction of bone marrow  
526 aspirates may have a positive effect on the anti-inflammatory process for their differentiation

527 and paracrine effects (L. Chen, Tredget, Wu, Wu, & Wu, 2008; Park, Ahn, Sung, Ahn, &  
528 Chang, 2018). Another important point was the large HPUC membrane water absorption  
529 capacity (shown in swelling tests). Better dressing water uptake could lead to different forms  
530 of exudate retention, which may cause changes in cytokine levels and growth factors on the  
531 wound surface and faster cicatrization (Yamane et al., 2015).

#### 532 **4. Conclusions**

533 This paper describes a study of synthesized chitosan/PLGA networks, which were found to  
534 present continuous degradation in aqueous solution. The hydrolytic degradation of  
535 polyurethane blocks liberated chitosan chains that dissolved in the aqueous solution. We  
536 confirmed that this biomaterial has low cytotoxicity and supports cell proliferation. The  
537 synthesis was based on unmodified chitosan and new crosslinkers consisting of a low  
538 molecular weight polyester polyurethane with NCO terminations, enabling crosslinking with  
539 free amine of chitosan. The use of BMMNCs helped to close the wounds, reduce  
540 inflammation and improve neovascularization around the wound. The results show that the  
541 synthesized hydrogel plus BMMNCs is suitable for use as a dressing for diabetic wounds and  
542 has a potential use in tissue engineering.

#### 543 **Acknowledgments**

544 The author is grateful to Gabriela Wentz for technical assistance in RMN analysis, also to the  
545 Nuclear Magnetic Resonance Laboratory - Regional Nanoscience and Nanotechnology  
546 Laboratory (LNNANO)

#### 547 **Funding:**

548 This work was funded by: Coordenação de Aperfeiçoamento de Pessoal de Nível Superior  
549 - doctoral fellowships to Viezzer, C (CAPES/PDSE-BEX: 1408/11- 9) and the Spanish Ministry  
550 of Economy and Competitiveness (MINECO) through the MAT2016-76039-C4-1-R Project,  
551 including FEDER financial support. CIBER-BBN is an initiative funded by the VI National  
552 R&D&i Plan 2008–2011, Iniciativa Ingenio 2010, Consolider Program, CIBER Actions and  
553 financed by the Instituto de Salud Carlos III with assistance from the European Regional  
554 Development Fund.

#### 555 **Reference**

556

557 Abused, W., Doe, J., Ad, G. R., Lo, B. I. O., Man, G.-H. U., Oach, A., ... Ward, G. (2014).

- 558 from the SAGE Social Science Collections . All Rights Reserved . *Journal of Composite*  
559 *Materials*, 16(4), 928–940. <https://doi.org/0803973233>
- 560 Ahmed, R., Tariq, M., Ali, I., Asghar, R., Noorunnisa Khanam, P., Augustine, R., & Hasan, A.  
561 (2018). Novel electrospun chitosan/polyvinyl alcohol/zinc oxide nanofibrous mats with  
562 antibacterial and antioxidant properties for diabetic wound healing. *International Journal*  
563 *of Biological Macromolecules*, 120, 385–393.  
564 <https://doi.org/10.1016/j.ijbiomac.2018.08.057>
- 565 Andrade, F., Goycoolea, F., Chiappetta, D. a., das Neves, J., Sosnik, A., & Sarmiento, B.  
566 (2011). Chitosan-Grafted Copolymers and Chitosan-Ligand Conjugates as Matrices for  
567 Pulmonary Drug Delivery. *International Journal of Carbohydrate Chemistry*, 2011, 1–14.  
568 <https://doi.org/10.1155/2011/865704>
- 569 Baltzis, D., Eleftheriadou, I., & Veves, A. (2014). Pathogenesis and Treatment of Impaired  
570 Wound Healing in Diabetes Mellitus: New Insights. *Advances in Therapy*, 31(8), 817–  
571 836. <https://doi.org/10.1007/s12325-014-0140-x>
- 572 Barikani, M., Honarkar, H., & Barikani, M. (2010). Synthesis and characterization of chitosan-  
573 based polyurethane elastomer dispersions. *Monatshefte Fur Chemie*, 141(6), 653–659.  
574 <https://doi.org/10.1007/s00706-010-0309-1>
- 575 Boulton, A. J. M. (2013). The pathway to foot ulceration in diabetes. *Medical Clinics of North*  
576 *America*, 97(5), 775–790. <https://doi.org/10.1016/j.mcna.2013.03.007>
- 577 Casettari, L., Vllasaliu, D., Castagnino, E., Stolnik, S., Howdle, S., & Illum, L. (2012).  
578 PEGylated chitosan derivatives: Synthesis, characterizations and pharmaceutical  
579 applications. *Progress in Polymer Science*, 37(5), 659–685.  
580 <https://doi.org/10.1016/j.progpolymsci.2011.10.001>
- 581 Chen, L., Tredget, E. E., Wu, P. Y. G., Wu, Y., & Wu, Y. (2008). Paracrine factors of  
582 mesenchymal stem cells recruit macrophages and endothelial lineage cells and enhance  
583 wound healing. *PLoS ONE*, 3(4). <https://doi.org/10.1371/journal.pone.0001886>
- 584 Chen, S. H., Tsao, C. T., Chang, C. H., Wu, Y. M., Liu, Z. W., Lin, C. P., ... Hsieh, K. H. (2012).  
585 Synthesis and characterization of thermal-responsive chitin-based polyurethane  
586 copolymer as a smart material. *Carbohydrate Polymers*, 88(4), 1483–1487.  
587 <https://doi.org/10.1016/j.carbpol.2012.01.055>
- 588 Ching Ting Tsao, Chih Hao Chang, Yu Dar Li, Ming Fung Wu, Chun Pin Lin, Jin Lin Han, ...  
589 Kuo Huang Hsieh. (2011). Development of chitosan/ dicarboxylic acid hydrogels as  
590 wound dressing materials. *Journal of Bioactive and Compatible Polymers*, 26(5), 519–  
591 536. <https://doi.org/10.1177/08839115111422627>
- 592 de Britto, D., & Campana-Filho, S. P. (2007). Kinetics of the thermal degradation of chitosan.  
593 *Thermochimica Acta*, 465(1–2), 73–82. <https://doi.org/10.1016/j.tca.2007.09.008>
- 594 de Moura, M. R., Aouada, F. a, & Mattoso, L. H. C. (2008). Preparation of chitosan



595 nanoparticles using methacrylic acid. *Journal of Colloid and Interface Science*, 321(2),  
596 477–483. <https://doi.org/10.1016/j.jcis.2008.02.006>

597 Dinh, T., Tecilazich, F., Kafanas, A., Doupis, J., Gnardellis, C., Leal, E., ... Veves, A. (2012).  
598 Mechanisms involved in the development and healing of diabetic foot ulceration.  
599 *Diabetes*, 61(11), 2937–2947. <https://doi.org/10.2337/db12-0227>

600 Eming, S. A., Martin, P., & Tomic-canic, M. (2014). STATE OF THE ART REVIEW Wound  
601 repair and regeneration : Mechanisms , signaling , and translation. *Science Translational*  
602 *Medicine*, 6(265), 265sr6. <https://doi.org/10.1126/scitranslmed.3009337>

603 Escobar Ivirico, J. L., Salmerón-Sánchez, M., Gómez Ribelles, J. L., & Monleón Pradas, M.  
604 (2009). Poly(L-lactide) networks with tailored water sorption. *Colloid and Polymer*  
605 *Science*, 287(6), 671–681. <https://doi.org/10.1007/s00396-009-2026-z>

606 Flory, P. J., & Rehner, J. (1943). Statistical mechanics of cross-linked polymer networks II.  
607 Swelling. *The Journal of Chemical Physics*, 11(11), 521–526.  
608 <https://doi.org/10.1063/1.1723792>

609 Gámiz-González, M. A., Vidaurre, A., & Gómez Ribelles, J. L. (2017). Biodegradable  
610 chitosan-poly( $\epsilon$ -caprolactone) dialdehyde copolymer networks for soft tissue  
611 engineering. *Polymer Degradation and Stability*, 138, 47–54.  
612 <https://doi.org/10.1016/j.polymdegradstab.2017.02.005>

613 García-Pacios, V., Costa, V., Colera, M., & Martín-Martínez, J. M. (2011). Progress in Organic  
614 Coatings Waterborne polyurethane dispersions obtained with polycarbonate of  
615 hexanediol intended for use as coatings. *Progress in Organic Coatings*, 71, 136–146.  
616 <https://doi.org/10.1016/j.porgcoat.2011.01.006>

617 García Cruz, Dunia M., Gomez Ribelles, J. L., & Salmerón Sánchez, M. (2008). Blending  
618 polysaccharides with biodegradable polymers. I. Properties of chitosan/polycaprolactone  
619 blends. *Journal of Biomedical Materials Research - Part B Applied Biomaterials*, 85(2),  
620 303–313. <https://doi.org/10.1002/jbm.b.30947>

621 García Cruz, Dunia Mercedes, Salmerón-Sánchez, M., & Gómez-Ribelles, J. L. (2012).  
622 Stirred flow bioreactor modulates chondrocyte growth and extracellular matrix  
623 biosynthesis in chitosan scaffolds. *Journal of Biomedical Materials Research - Part A*,  
624 100 A(9), 2330–2341. <https://doi.org/10.1002/jbm.a.34174>

625 Heux, L., Brugnerotto, J., Desbrières, J., Versali, M. F., & Rinaudo, M. (2000). Solid state  
626 NMR for determination of degree of acetylation of chitin and chitosan.  
627 *Biomacromolecules*, 1(4), 746–751.

628 Hilfiker, A., Kasper, C., Hass, R., & Haverich, A. (2011). Mesenchymal stem cells and  
629 progenitor cells in connective tissue engineering and regenerative medicine: Is there a  
630 future for transplantation? *Langenbeck's Archives of Surgery*, 396(4), 489–497.  
631 <https://doi.org/10.1007/s00423-011-0762-2>

- 632 Hilmi, A. B. M., Halim, A. S., Hassan, A., Lim, C. K., Noorsal, K., & Zainol, I. (2013). In vitro  
633 characterization of a chitosan skin regenerating template as a scaffold for cells cultivation.  
634 *SpringerPlus*, 2(2002), 79. <https://doi.org/10.1186/2193-1801-2-79>
- 635 Hu, Y., Liu, Y., Qi, X., Liu, P., Fan, Z., Li, S. (2012) Novel bioresorbable hydrogels prepared  
636 from chitosan-graft-poly(lactide) copolymers. *Polym. Int*, 61, 74-81.  
637 <https://doi.org/10.1002/pi.3150>
- 638 Jiang, T., Nukavarapu, S. P., Deng, M., Jabbarzadeh, E., Kofron, M. D., Doty, S. B., ...  
639 Laurencin, C. T. (2010). Chitosan-poly(lactide-co-glycolide) microsphere-based  
640 scaffolds for bone tissue engineering: In vitro degradation and in vivo bone regeneration  
641 studies. *Acta Biomaterialia*, 6(9), 3457–3470.  
642 <https://doi.org/10.1016/j.actbio.2010.03.023>
- 643 Jiang, X., Li, J., Ding, M., Tan, H., Ling, Q., Zhong, Y., & Fu, Q. (2007). Synthesis and  
644 degradation of nontoxic biodegradable waterborne polyurethanes elastomer with  
645 poly(ε-caprolactone) and poly(ethylene glycol) as soft segment. *European Polymer*  
646 *Journal*, 43(5), 1838–1846. <https://doi.org/10.1016/j.eurpolymj.2007.02.029>
- 647 Jovanovic, D., Engels, G. E., Plantinga, J. a., Bruinsma, M., Van Oeveren, W., Schouten, a.  
648 J., ... Harmsen, M. C. (2010). Novel polyurethanes with interconnected porous structure  
649 induce in vivo tissue remodeling and accompanied vascularization. *Journal of*  
650 *Biomedical Materials Research - Part A*, 95(1), 198–208.  
651 <https://doi.org/10.1002/jbm.a.32817>
- 652 Koehler, J., Brandl, F. P., & Goepferich, A. M. (2018). Hydrogel wound dressings for bioactive  
653 treatment of acute and chronic wounds. *European Polymer Journal*, 100(December  
654 2017), 1–11. <https://doi.org/10.1016/j.eurpolymj.2017.12.046>
- 655 Kuo, Y. R., Wang, C. T., Cheng, J. T., Wang, F. S., Chiang, Y. C., & Wang, C. J. (2011). Bone  
656 marrow-derived mesenchymal stem cells enhanced diabetic wound healing through  
657 recruitment of tissue regeneration in a rat model of streptozotocin-induced diabetes.  
658 *Plastic and Reconstructive Surgery*, 128(4), 872–880.  
659 <https://doi.org/10.1097/PRS.0b013e3182174329>
- 660 Leventis, N., Sotiriou-Leventis, C., Chandrasekaran, N., Mulik, S., Larimore, Z. J., Lu, H., ...  
661 Mang, J. T. (2010). Multifunctional polyurea aerogels from isocyanates and water. A  
662 structure-property case study. *Chemistry of Materials*, 22(24), 6692–6710.  
663 <https://doi.org/10.1021/cm102891d>
- 664 Marchant, R. E., Zhao, Q., Anderson, J. M., & Hiltner, A. (1987). Degradation of a poly(ether  
665 urethane urea) elastomer: infra-red and XPS studies. *Polymer*, 28(12), 2032–2039.  
666 [https://doi.org/10.1016/0032-3861\(87\)90037-1](https://doi.org/10.1016/0032-3861(87)90037-1)
- 667 Marcos-Fernández, A., Abraham, G. A., Valentín, J. L., & Román, J. S. (2006). Synthesis  
668 and characterization of biodegradable non-toxic poly(ester-urethane-urea)s based on

- 669 poly( $\epsilon$ -caprolactone) and amino acid derivatives. *Polymer*, 47(3), 785–798.  
670 <https://doi.org/10.1016/j.polymer.2005.12.007>
- 671 Masson-Meyers, D. S., Bumah, V. V., & Enwemeka, C. S. (2016). A comparison of four  
672 methods for determining viability in human dermal fibroblasts irradiated with blue light.  
673 *Journal of Pharmacological and Toxicological Methods*, 79, 15–22.  
674 <https://doi.org/10.1016/j.vascn.2016.01.001>
- 675 Merchant, Z., Taylor, K. M. G., Stapleton, P., Razak, S. a., Kunda, N., Alfagih, I., ...  
676 Somavarapu, S. (2014). Engineering hydrophobically modified chitosan for enhancing  
677 the dispersion of respirable microparticles of levofloxacin. *European Journal of*  
678 *Pharmaceutics and Biopharmaceutics*, 88(3), 816–829.  
679 <https://doi.org/10.1016/j.ejpb.2014.09.005>
- 680 Moise, M., Sunel, V., Holban, M., Popa, M., Desbrieres, J., Peptu, C., & Lionte, C. (2012).  
681 Double crosslinked chitosan and gelatin submicronic capsules entrapping aminoacid  
682 derivatives with potential antitumoral activity. *Journal of Materials Science*, 47(23), 8223–  
683 8233. <https://doi.org/10.1007/s10853-012-6719-1>
- 684 Neto, C. G. T., Giacometti, J. a., Job, a. E., Ferreira, F. C., Fonseca, J. L. C., & Pereira, M.  
685 R. (2005). Thermal analysis of chitosan based networks. *Carbohydrate Polymers*, 62(2),  
686 97–103. <https://doi.org/10.1016/j.carbpol.2005.02.022>
- 687 Oberyszyn, T. M. (2008). *Department of Pathology, The Ohio State University, Columbus, OH*  
688 *43210*. (8), 2993–2999.
- 689 Ouyang, Q. Q., Hu, Z., Lin, Z. P., Quan, W. Y., Deng, Y. F., Li, S. D., ... Chen, Y. (2018).  
690 Chitosan hydrogel in combination with marine peptides from tilapia for burns healing.  
691 *International Journal of Biological Macromolecules*, 112, 1191–1198.  
692 <https://doi.org/10.1016/j.ijbiomac.2018.01.217>
- 693 Page, J. M., Prieto, E. M., Dumas, J. E., Zienkiewicz, K. J., Wenke, J. C., Brown-Baer, P., &  
694 Guelcher, S. a. (2012). Biocompatibility and chemical reaction kinetics of injectable,  
695 settable polyurethane/allograft bone biocomposites. *Acta Biomaterialia*, 8(12), 4405–  
696 4416. <https://doi.org/10.1016/j.actbio.2012.07.037>
- 697 Park, W. S., Ahn, S. Y., Sung, S. I., Ahn, J. Y., & Chang, Y. S. (2018). Strategies to enhance  
698 paracrine potency of transplanted mesenchymal stem cells in intractable neonatal  
699 disorders. *Pediatric Research*, 83(1–2), 214–222. <https://doi.org/10.1038/pr.2017.249>
- 700 Pérez-Limiñana, M. A., Arán-Aís, F., Torró-Palau, A. M., Orgilés-Barceló, a. C., & Martín-  
701 Martínez, J. M. (2005). Characterization of waterborne polyurethane adhesives  
702 containing different amounts of ionic groups. *International Journal of Adhesion and*  
703 *Adhesives*, 25(6), 507–517. <https://doi.org/10.1016/j.ijadhadh.2005.02.002>

- 704 Pretsch, T., Jakob, I., & Müller, W. (2009). Hydrolytic degradation and functional stability of  
705 a segmented shape memory poly(ester urethane). *Polymer Degradation and Stability*,  
706 94(1), 61–73. <https://doi.org/10.1016/j.polymdegradstab.2008.10.012>
- 707 Rowlands, a. S., Lim, S. a., Martin, D., & Cooper-White, J. J. (2007). Polyurethane/poly(lactic-  
708 co-glycolic) acid composite scaffolds fabricated by thermally induced phase separation.  
709 *Biomaterials*, 28(12), 2109–2121. <https://doi.org/10.1016/j.biomaterials.2006.12.032>
- 710 Sayed, O. N., Abdel-Rahman, R. M., Pavliňák, D., Abdel-Mohsen, A. M., Jancar, J., Burgert,  
711 L., ... Fohlerova, Z. (2016). Wound dressing based on chitosan/hyaluronan/nonwoven  
712 fabrics: Preparation, characterization and medical applications. *International Journal of*  
713 *Biological Macromolecules*, 89, 725–736. <https://doi.org/10.1016/j.ijbiomac.2016.04.087>
- 714 Subramani, S., Park, Y., Lee, Y., & Kim, J. (2003). *New development of polyurethane*  
715 *dispersion derived from blocked aromatic diisocyanate*. 48, 71–79.  
716 [https://doi.org/10.1016/S0300-9440\(03\)00118-8](https://doi.org/10.1016/S0300-9440(03)00118-8)
- 717 Tao, Z., Shi, A., & Zhao, J. (2015). Epidemiological Perspectives of Diabetes. *Cell*  
718 *Biochemistry and Biophysics*, 73(1), 181–185. [https://doi.org/10.1007/s12013-015-](https://doi.org/10.1007/s12013-015-0598-4)  
719 [0598-4](https://doi.org/10.1007/s12013-015-0598-4)
- 720 Ünlü, C.H., Pollet, E., Avérous, L., Original Macromolecular Architectures Based on poly( $\epsilon$ -  
721 caprolactone) and poly( $\epsilon$ -thiocaprolactone) Grafted onto Chitosan Backbone (2018) *Int.*  
722 *J. Mol. Sci.* 19, 3799. <https://doi:10.3390/ijms19123799>
- 723 Velazquez-Morales, P., Le Nest, J.-F., & Gandini, A. (1998). Polymer electrolytes derived from  
724 chitosan/polyether networks. *Electrochimica Acta*, 43(10–11), 1275–1279.  
725 [https://doi.org/10.1016/S0013-4686\(97\)10030-5](https://doi.org/10.1016/S0013-4686(97)10030-5)
- 726 Wang, W., Ping, P., Chen, X., & Jing, X. (2006). Polylactide-based polyurethane and its  
727 shape-memory behavior. *European Polymer Journal*, 42(6), 1240–1249.  
728 <https://doi.org/10.1016/j.eurpolymj.2005.11.029>
- 729 Yamane, T., Nakagami, G., Yoshino, S., Shimura, M., Kitamura, A., Kobayashi-Hattori, K., ...  
730 Sanada, H. (2015). Hydrocellular foam dressings promote wound healing associated  
731 with decrease in inflammation in rat periwound skin and granulation tissue, compared  
732 with hydrocolloid dressings. *Bioscience, Biotechnology and Biochemistry*, 79(2), 185–  
733 189. <https://doi.org/10.1080/09168451.2014.968088>
- 734 Zawadzki, J., & Kaczmarek, H. (2010). Thermal treatment of chitosan in various conditions.  
735 *Carbohydrate Polymers*, 80(2), 395–401. <https://doi.org/10.1016/j.carbpol.2009.11.037>
- 736 Zhang, Shubiao, Cheng, L., & Hu, J. (2003). NMR studies of water-borne polyurethanes.  
737 *Journal of Applied Polymer Science*, 90(1), 257–260. <https://doi.org/10.1002/app.12696>
- 738 Zhang, S., Ren, Z., He, S., Zhu, Y., & Zhu, C. (2007). FTIR spectroscopic characterization of  
739 polyurethane-urea model hard segments (PUUMHS) based on three diamine chain  
740 extenders. *Spectrochimica Acta - Part A: Molecular and Biomolecular Spectroscopy*,

741 66(1), 188–193. <https://doi.org/10.1016/j.saa.2006.02.041>

742

743 Zuber, M., Zia, K. M., Mahboob, S., Hassan, M., & Bhatti, I. A. (2010). Synthesis of chitin-  
744 bentonite clay based polyurethane bio-nanocomposites. *International Journal of*  
745 *Biological Macromolecules*, 47(2), 196–200.  
746 <https://doi.org/10.1016/j.ijbiomac.2010.04.022>

747

748